JOURNAL OF MATERIALS SCIENCE 10 (1975) 12–24

Fracture toughness and mechanical behaviour of an epoxy resin

K. SELBY, L. E. MILLER
Department of Materials Technology, University of Technology, Loughborough, Leicestershire, UK

The variation of fracture and mechanical properties of epoxy resin Epikote 828, cured with diaminodiphenyl-methane by variation of the resin/amine ratio has been determined. Observations of the crack tip have shown that fracture toughness variations can be attributed to the different blunting characteristics of the various resin/amine compositions. A systematic variation in the thermal transitions of the resins also occurs as a function of composition. Investigations by chemical etching and small angle X-ray scattering have failed to reveal a structural entity which can be invoked to explain the trends in fracture and mechanical properties.

It has been found that care must be taken when choosing the method of evaluation of fracture parameters in order that meaningful comparisons can be made between different resin compositions.

1. Introduction

It has already been noted [1] that the fracture surface energy (FSE) of an epoxy resin is dependent upon the relative amounts of resin and crosslinking agent employed. The usual behaviour of cured epoxy resins in double-cantilever-beam cleavage tests is described as crack jumping [1, 2]. This behaviour can be contrasted with that of other rigid polymeric materials, particularly amorphous thermoplastics which usually exhibit continuous tearing during such tests. (Normally, test conditions are (a) room temperature (b) testing machine crosshead speeds in the range 1.0 to 10 mm min^{-1} [3, 4]). The purpose of the work reported here was to establish

(a) how the variation in resin/crosslink agent ratio affects the values of FSE, plane strain fracture toughness (K_{IC}) and other mechanical properties

(b) how different methods of evaluating fracture parameters affect the numerical result

(c) whether or not the variation in fracture and mechanical behaviour can be attributed to a systematic structural or network change.

Investigations were made with the aid of the following techniques:

(a) tapered double-cantilever-beam (TDCB) fracture toughness tests

(b) analysis of test data by (i) Berry's method [5] (ii) Irwin-Kies equation [6] (iii) area under load-extension curve [7, 8].

(c) Chemical etching, optical microscopy, thermomechanical (penetrometer) tests and small angle X-ray scattering.

2. Preparation and testing

A commercial diglycidol ether of bisphenol-A epoxy resin, Epikote 828, was used, together with 4-4′-diamino-diphenyl-methane (DDM) as cross-linking agent. The resin has the formula

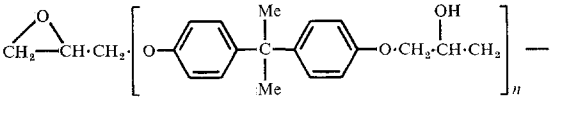

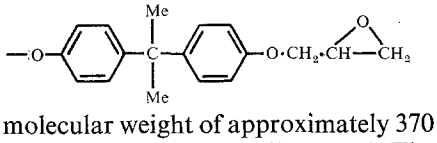

and has a molecular weight of approximately 370 (thus n lies between 1 and 3 for Epikote 828). The crosslinking agent has the formula

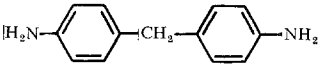

Various ratios of 828/DDM were made up and cured as indicated in Table I. Resin at 80°C and

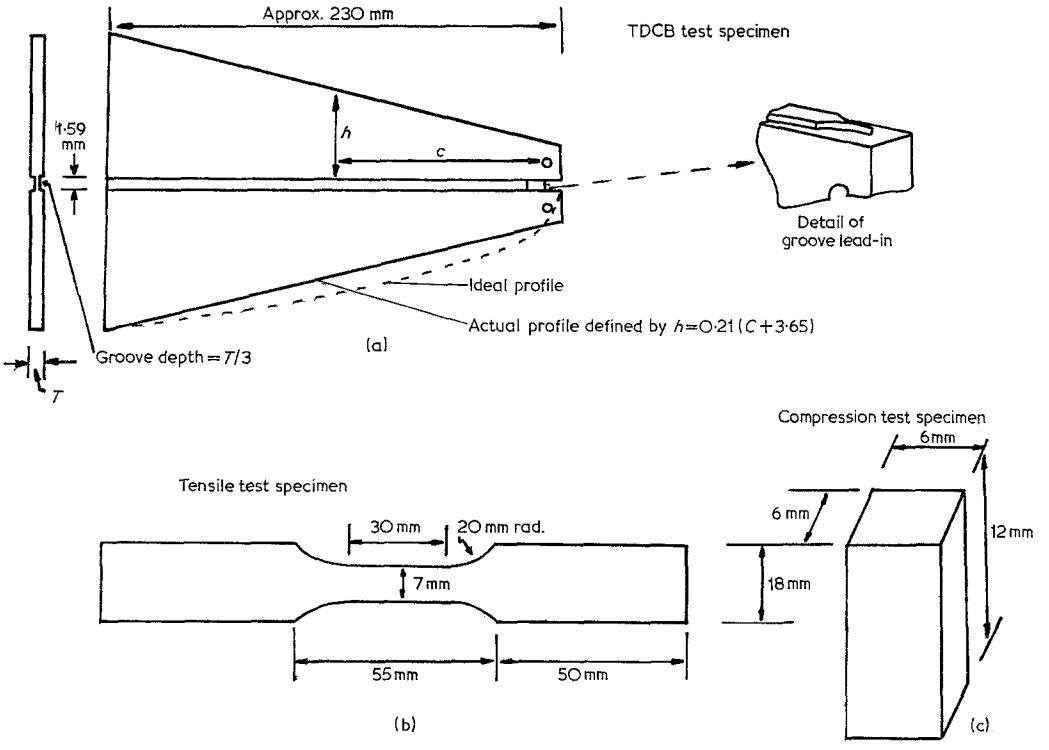

Figure 1 Test piece geometries (a) TDCB fracture-toughness test piece, (b) tensile test piece and (c) compression test piece.

DDM at 110°C were mixed and de-gassed prior to casting into steel moulds which had been pre-heated to 100°C. The temperature of the curing mixture was monitored by a thermocouple inserted through the top of the mould. On completion of the appropriate cure cycle, the mould was allowed to cool, in still air, to room temperature before removal of the sheet of cured resin. TDCB fracture toughness test pieces were machined from the 6 mm thick sheets of cured resin, the geometry of the test piece being defined in Fig. 1a. Tensile and compression test pieces were also machined from the cured resin and their geometries are also shown in Fig. 1. Samples were taken for etching and small angle X-ray scattering experiments and also for determination of transition temperatures by a penetrometer method.

All mechanical tests were done in an Instron TTM (floor model) machine, the majority of tests being carried out at 0.1 mm min^{-1} cross-head speed. Tensile modulus measurements were made with the aid of an Instron 0-10% strain gauge extensometer and penetrometer tests were carried out in a Dupont instrument. Small angle X-ray scattering experiments employed a Rikagu Denki 2202 goniometer with Cu$K\alpha$ radiation (100 second counts, step scanning between $2\theta = 0.55°$ and $\sim 1.0°$ in 0.01° intervals). Etching was carried out by immersion in chromic acid and mixed chromic, phosphoric and sulphuric acids of varying proportions. Temperatures between 70 and 100°C and times from 2 min to 2 h were used. Subsequent examination was on a Riechert projection microscope. Some fracture surfaces were examined in a Cambridge Stereoscan electron microscope.

3. Evaluation of fracture parameters

While it is not intended to explain in detail how the tests were conducted, it is worth considering what data can be obtained from fracture toughness tests and how it can be manipulated in a simple manner to provide values of FSE and K_{IC}.

In essence, the cleavage test, developed by several workers [5, 9-15] over a period of time, consists in propagating a crack through a material in such a way that its direction of motion is controlled. The parameters load,

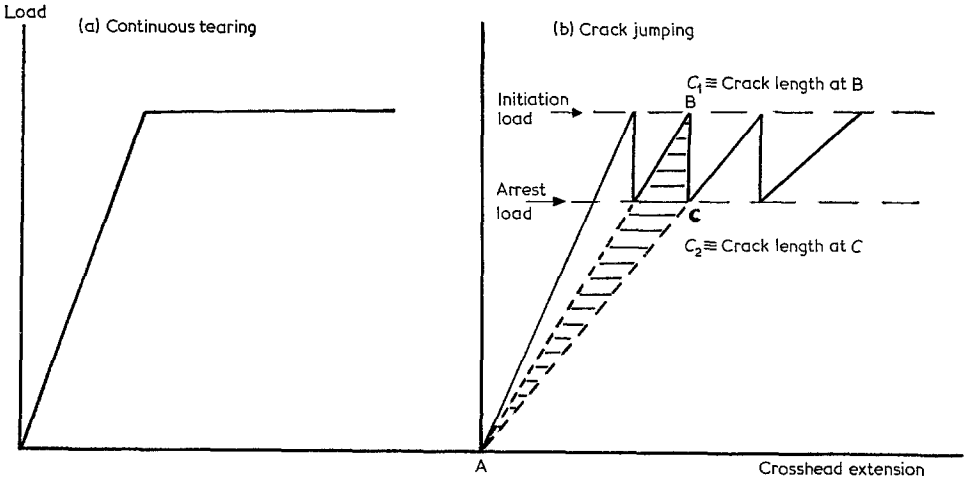

Figure 2 Idealized load-extension plots for TDCB specimens in (a) continuous tearing and (b) crack-jumping modes.

TABLE I Casting composition and cure details for Epikote 828/Epikure DDM epoxy resin system

Cast number	DDM content parts (by weight)	Cure cycle
12	27	1 h at 100°C + 2 h 100 ↑ 175°C
13	27	as above
14	27	as above
15	20	as above
16	30	as above
17	20	as above
18	30	as above
19	35	as above
20	40	as above
21	20	as above
22	27	1 h at 100°C + 2 h 100 ↑ 175°C + 0.5 h at 175°C
23	27	1 h at 100°C + 2 h 100 ↑ 175°C + 1 h at 175°C
24	27	1 h at 100°C + 2 h 100 ↑ 175°C
25	27	as above
26	27	as above
27	27	as above
28	27	1 h at 100°C + 2 h 100 ↑ 175°C + 1.6h at 175°C

Casts 22, 23, 28 were used to investigate the effect of cure time at 175°C.
Casts 25, 26 and 27 were used to investigate the effect of faster rates of testing.
↑ indicates that the 2 h "at 175°C" in subsequent figure captions is only a nominal description. In each case, the resin took approximately 1.75 h to reach 175°C after increasing the temperature of the curing oven from 100°C.

crack length, end deflection and latterly, near-tip crack opening displacement (COD) are measured during the test. Control of the crack direction is usually achieved by machining grooves along the sides of the specimen as indicated in Fig. 1. [5]. Several methods of processing fracture test data are available [4-7, 16] but in this case, three well-known variants which do not involve calibration tests or extensive computation were employed.

3.1. Berry's method

By invoking beam theory and postulating that the deflection behaviour of a DCB test piece conforms to an equation of the form

$$f = (ac^{-n})\delta \qquad (1)$$

where f = load on specimen, a = constant, n = constant, c = crack length, $\delta/2$ = end deflection of one half of the DCB specimen, Berry [5] has established that plots of log f/δ versus log C and of $f\delta/w$ versus c (w being the width of the crack plane) should be linear. From the slopes of the two plots, a value for FSE can be obtained

$$\text{FSE} = \gamma = \frac{\text{slope 1} \times \text{slope 2}}{4} = \frac{nm}{4}. \qquad (2)$$

The well-known relationship between FSE, Young's modulus E, strain energy release rate G, and K_c is

$$K_c^2 = EG_c = 2E\gamma\ . \qquad (3)$$

Thus, knowing E and γ, K_c can be found. By referring to Fig. 2 it can be seen that K_c can be interpreted as an initiation, a propagation or an arrest parameter. This is because (a) maximum loads in the crack jumping situation and loads

for "equilibrium" tearing (zero crack speed) [14] are those appertaining to the initiation of crack movement, (b) loads for non-zero (but uniform) crack velocity in the tearing mode are in practice related to a dynamic situation, with crack-tip conditions differing from the "equilibrium" case and (c) minimum loads in the crack jumping situation are relevant to the situation when a crack just stops.

3.2. Irwin-Kies equation

One form of the equation developed by Irwin and Kies [6] is

$$2\gamma = G_c = \tfrac{1}{2} \cdot \frac{f^2}{w} \cdot \frac{dR}{dC} \qquad (4)$$

where R is the compliance of the specimen (deflection per unit load). Thus if a plot of R versus C is drawn for any specimen geometry, its slope at a particular value of f and C, (and hence a particular value of (R and C), can be measured and G_c can be evaluated. It is to be noted that a linear plot of R versus C would be advantageous. This can be achieved by designing the test piece such that the compliance decreases as crack length increases. To a first approximation, the equation [17]

$$\frac{dR}{dC} = \left(\frac{3C^2}{h^3} + \frac{1}{h}\right) \frac{8}{EB} \qquad (5)$$

(where h = half height of the complete DCB specimen and B = gross thickness of the specimen) defines such a geometry (see Fig. 1a). Equation 5, deduced from simple beam theory, defines a cubic profile, but in practice it is found that a straight-edged, tapered test piece will produce an approximately linear R versus C plot.

3.3. Area under load-extension curve method

Referring to Fig. 2, it can be seen that the shaded area ABC represents the amount of stored elastic energy in the system machine + specimen which was expended during the propagation of the crack from a length C_1 to C_2. If this area is measured and converted accordingly to an energy value, then a figure for FSE can be obtained by dividing the energy by the total area of fracture surface created during the C_1 to C_2 jump. The same concept can be applied to a tearing mode.

At this point it is informative to consider the significance of the values of FSE (or fracture surface work as it is sometimes known) that can be obtained by the three methods outlined above. In principle, all three methods should give the same result, provided that the crack propagates at the same constant speed. FSE in this context is therefore a propagation value. It is well established [3, 18] that FSE can vary with crack speed. For materials which exhibit continuous tearing modes of failure at normal crosshead speeds, it is to be expected that all three methods would yield the same value of γ. However, materials which undergo crack jumping will necessarily have been subject to varying crack speeds. Therefore any area under curve method of measurement associated with increases in crack length by jumping will give an undefined mean value of FSE. The range of crack speeds during a crack jump will influence the weighting of this mean value. The methods which employ peak loads and initiation crack lengths, however, would be expected to agree under crack jumping situations. This also applies to crack arrest values. The above comments should serve to illustrate one of the interpretation problems of fracture mechanics. For example, how does one interpret FSE as an initiation or arrest parameter when a basic requirement for its evaluation is that fracture surface be generated? Strictly, a complete view of the fracture problem can only be obtained by considering macroscopic and microscopic parameters in combination.

Given that the engineering interpretation of fracture data is still a subject of considerable debate, it is nevertheless valid to use such data for comparative purposes such as the present work on epoxy resins requires.

4. Results and discussion

4.1. Fracture and mechanical properties

All resins containing greater than 20 parts of DDM per 100 parts of resin by weight failed by crack jumping. In specimens containing 20 parts DDM, tearing was observed between crack lengths of approximately 0.03 m and 0.08 m. Crack jumping was predominant at other crack lengths. A peak in the γ versus DDM content curve (Fig. 3) was obtained at approximately 35 parts DDM per 100 parts resin. The relative height of the peak varied according to the method of calculation, as indicated in the figure. Statistical data concerning the various methods of calculation are given in Appendix 1. Fig. 4 shows how the tensile and compressive Young's moduli varied with DDM content. It is

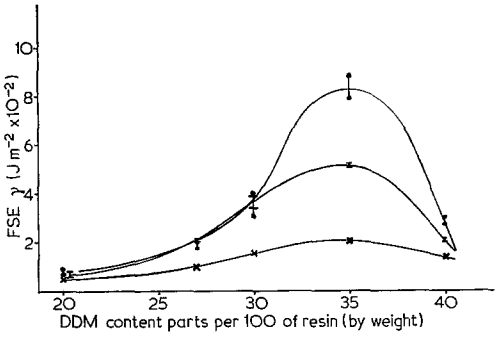

Figure 3 Fracture surface energy (FSE, γ) versus DDM content for Epikote 828/Epikure DDM cured 1 h at 100°C, 2 h at 175°C (nominal).
I – range of values obtained by Berry's method;
I – range of values obtained by Irwin-Kies equation;
× – average value for several crack propagation steps in more than one specimen by area method. Values obtained by Berry's method and Irwin-Kies equation represent "combined-plots", as indicated in Appendix I, by statistical means and manual graph plotting.

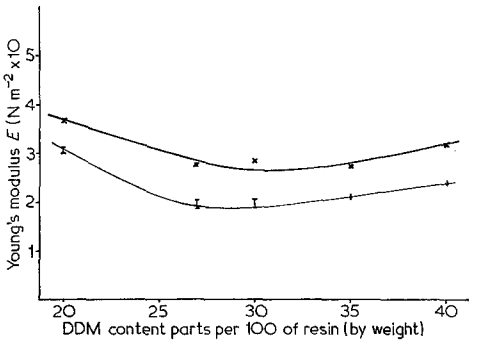

Figure 4 Tensile and compressive Young's Modulus, E, versus DDM content for Epikote 828/Epikure DDM cured 1 h at 100°C 2 h at 175°C (nominal).
× – compressive modulus (average of 2 values, minimum);
I – tensile modulus;
+ – tensile modulus (single values).

worth noting that the lowest DDM content gave the highest tensile modulus and that the nominal stoichiometric ratio (100/27:828/DDM) gave the lowest figure. This was an unexpected result. A similar trend for compressive modulus was observed, although the exact values of the tensile moduli fell below those of the compressive moduli in all cases. Table II endorses the unexpected behaviour, illustrating the variation of compressive yield stress and 1% proof stress (compressive) with DDM content. 1% proof stress appears to be more sensitive to hardener content variation than does yield stress. A definite yield drop in compression was not

TABLE II Tensile and compressive test data for Epikure 828/Epikure DDM resin system

Cast number	DDM content parts (by weight)	Ultimate tensile strength ($\times 10^{-6}$ N m^{-2})	Fracture stress ($\times 10^{-6}$ N m^{-2})	Comments on tensile stress-strain behaviour	Compressive yield stress ($\times 10^{-6}$ N m^{-2})	Compressive proof stress ($\times 10^{-6}$ N m^{-2})
15, 21	20	95, 96	—	Deviation from linearity. Load drop prior to failure.	125	123
17	20	—	73, 80	Almost complete linearity. No load drop prior to failure.		
14	27	—	78, 67	Some deviation from linearity.	—	85
13	27	—	73, 66	No load drop prior to failure.		
12	27	—	71	Deviation not as great as for 30 parts DDM specimens.		
16	30	—	83, 81	Deviation from linearity near top of load-extension		
18	30	—	83, 78	curve. No load drop prior to failure.	109	88
19	35	82, 81	—	Deviation from linearity. Load drop prior to failure.	105	94
20	40	84, 85	—	as above	104	98

Where a load-drop prior to failure was observed, a UTS based on original area of cross-section has been quoted. Where this did not occur, a fracture stress based on original area has been quoted.
Linearity in this context refers to the major portion of the load-extension curve and does not imply a perfect straight line plot.

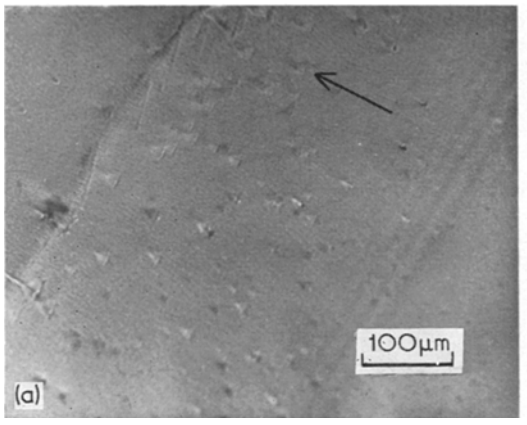

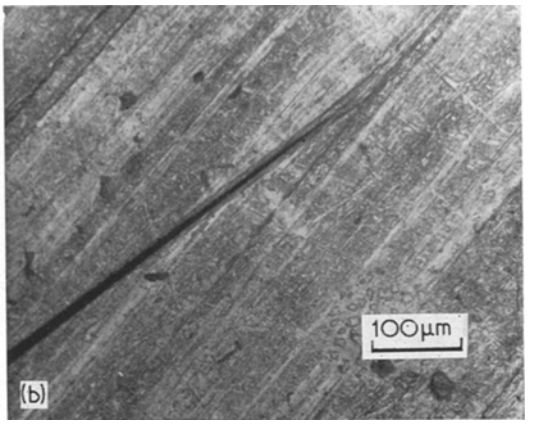

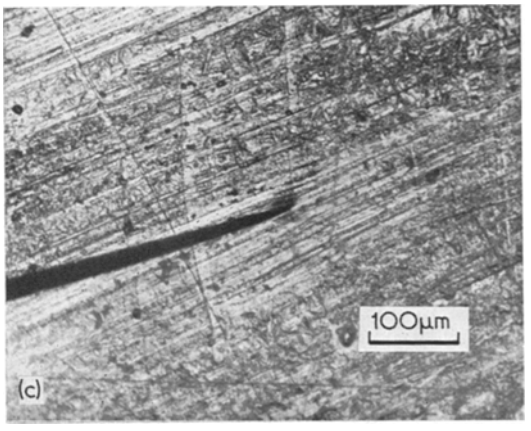

Figure 5 (*a*) Optical micrograph of arrest location on a small cleavage specimen tested *in situ* on the Reichert microscope. Cast 17, 20 parts DDM. Arrow indicates direction of crack propagation. (b) Side view of crack, propagated through a small cleavage specimen of cast 17, 20 parts DDM. (c) As (b), cast 16, 30 parts DDM.

observed in the specimen of stoichiometric composition.

Table II also contains information about the tensile behaviour of the resin. Note that two of the 20 parts DDM specimens fractured prior to any load drop or deviation from linearity, whereas all other tensile specimens exhibited deviation from linearity. Note also that a maximum load, followed by a load-drop, was evident only at 20, 35 and 40 parts DDM.

Values of plane strain fracture toughness are given in Table III. The existence of a maximum value at approximately 35 parts DDM is evident, although the relative value of the maximum when compared to the minimum figure is less than for the γ versus DDM relationship of Fig. 3. Table IV summarizes the effect of

TABLE III Plane strain fracture toughness, K_{IC}, of Epikote 828/Epikure DDM versus DDM content

Cast number	DDM content parts (by weight)	Plane strain fracture toughness K_{IC} ($\times 10^{-5}$ N $m^{-3/2}$)
17, 21	20	6.6
12, 13, 14	27	9.0
16, 18	30	12.5
19	35	14.7
20	40	9.0

crosshead speed on the various mechanical properties of the stoichiometric resin.

Ancillary investigations concerning the behaviour of the material at the crack tip were carried out by propagating cracks through small DCB specimens in a jig attached to the stage of the Reichert microscope. A wedge load was applied to the pre-cracked end of the specimen and photographs were taken at various degrees of strain. The main conclusion from this work was that considerable blunting occurred at the crack tip in resins of 27 to 40 parts DDM. A similar effect has been observed for Araldite CT200 cured with HT901 [19]. The 20 parts DDM specimens would not accommodate significant strain at the crack tip prior to a sudden propagation. (Significant crack jumping was readily observed in 20 parts DDM small cleavage specimens, whereas the large TDCB specimens tended to fail by tearing or very small crack jumps.This is a geometry/strain rate effect). The small DCB specimens, although not yielding any quantitative results, served to illustrate differences in crack-tip behaviour, especially during the initial and final stages of a crack jump. For

TABLE IV Fracture properties and mechanical properties of Epikote 828/Epikure DDM of stoichiometric proportion versus testing speed

Cast number	DDM content parts (by weight)	FSE γ	$K_{IC} \times 10^{-5}$ (N m$^{-3/2}$)	$E \times 10^{-9}$ (N m^{-2})	Rough zone size (mm)	Crosshead speed (mm min^{-1})
12, 13, 14	27	100 206	9.0	1.9–2.05	0.15–0.30	0.1
24, 25, 26, 27	27	91 156	8.1	2.06–2.14	0.07–0.16	1.0
24, 25, 26, 27	27	87 126	7.3	2.08–2.22	0.02–0.14	10.0

First figure in FSE column obtained from area under load extension curve. Second figure (higher values) from Irwin-Kies equation (combined plots see Table AI).
Rough zone sizes measured at equivalent crack lengths in the different specimens.

example, the triangular features shown in Fig. 5a and the near-tip region in Fig. 5b are at corresponding locations of a 100/20:828/DDM cleavage specimen (small type). A zone of deformation can be seen around the crack tip. The zone extends some distance along the propagation zone. This is to be contrasted with the situation at the tip of a crack in the 100/30: 828/DDM material (Fig. 5c). In this case, although the deformation appears to be limited to a small volume of material, the blunting of the tip is quite pronounced. The material, therefore, has a high initiation K_{IC}. It is also evident, from the behaviour of the tougher specimens during crack blunting, that the rough zones, as illustrated in Fig. 7, were the result of simultaneous growth of cracks on several crack planes. The inability of the low DDM-content material to sustain large crack-opening displacements at the crack tip prior to propagation is consistent with its low fracture toughness value. Observation during testing on the microscope jig revealed that the tip regions in the toughest resins were extensively deformed, allowing a considerable amount of crack blunting to occur. This was not the case for the 20 parts DDM material. This is in keeping with its observed higher modulus, since the tensile fracture stresses for all the resins are similar. A lower strain at failure might be expected for the material with the higher modulus. If the crack tip in considered as a region composed of miniature tensile specimens, the small crack opening displacement at the crack tip observed in the 20 parts DDM resin is to be expected.

4.2. Thermal properties

Fig. 6 shows how the transition temperatures varied with DDM content. The presence of two distinct transitions at low and high DDM contents, but only one at intermediate compositions, is worthy of note.

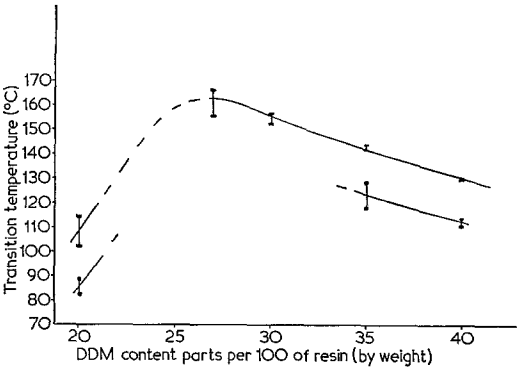

Figure 6 Variation of temperatures of transition with DDM content in Epikote 828/Epikure DDM cured 1 h at 100°C, 2 h at 175°C (nominal).

4.3. Microscopy of fracture surfaces

Optical and scanning electron microscopy revealed a variation in fracture surface features, according to whether the resin contained 20 parts DDM or greater than this amount. Apart from the lengths of the crack jumps, there were no apparent differences between the features on fracture surfaces of resins containing 27, 30, 35 and 40 parts DDM. The 20 parts DDM material did not show significant roughening at arrest points, and in fact, the arrest points were sometimes difficult to locate.

Examples of typical fracture surface features are shown in Figs. 7 and 8. The points of interest are:

(a) the nature of the transition from one crack-jump to the next, in specimens showing arrest points

(b) the relatively featureless surface comprising the majority of the propagation zone

(c) the multiplicity of fracture planes within the rough zone

(d) the existence of curved features in the smoother areas of fracture, (referred to as layer-lines in the remainder of this text)

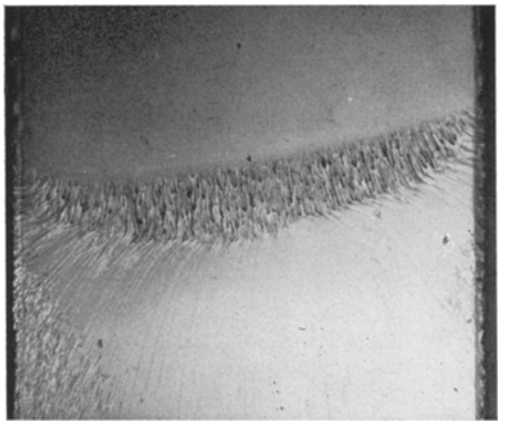

Figure 7 Overall view of arrest location in Epikote 828/Epikure DDM TDCB specimen. Reflected light. Cast 14, 27 parts DDM × 50.

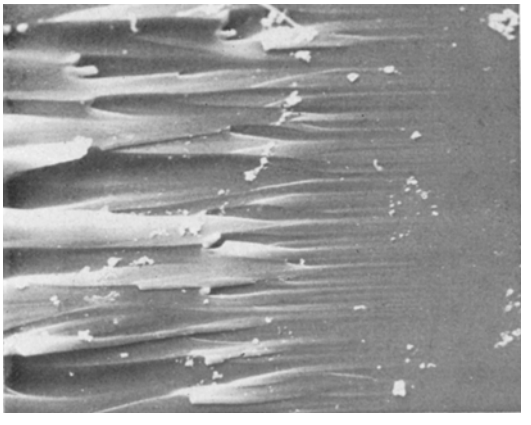

Figure 8 Stereoscan photograph of transition from smooth zone of a previous crack jump to rough zone of successive crack jump. Epikote 828/Epikure DDM. Cast 16, 30 parts DDM × 700. TDCB specimen.

(e) the sharp angular displacement between rough and smooth regions on the advancing slide of the rough zone

(f) the crescent shape of the rough zone itself

(g) the absence of macroscopically rough zones from the 20 DDM specimens.

Considering some of these points in a little more detail, it appears from Fig. 7 that a step change occurs at the arrest point, whereas Fig. 8 gives one the impression that a gradual transition has occurred. This is informative in that it illustrates the importance of using more than one microscopy technique for characterising the fracture surface whenever possible. While it has been stated that the major part of the propagation is macroscopically featureless, there are a significant number of "brush-marks" [20]. The exact mechanism of failure is not known at present and no hypothesis can be advanced for the formation of such markings. It was noticed that in some samples the "layer-lines" reappeared at irregular intervals along the fast-propagation zone and that their origins could, in some cases, be linked with a discontinuity such as an inclusion or possibly an air bubble in the casting. One interesting fracture surface feature in 20 parts DDM samples viewed by optical methods was the appearance of the numerous $\sim$ 8 μm-size triangular features in the vicinity of an arrest location. These may be associated with a craze-type phenomenon, Fig. 5a illustrates these features.

4.4. Chemical etching

Chemical etching of all compositions revealed essentially two kinds of feature, as shown in Figs. 9 and 10. It was found to be experimentally difficult to obtain an evenly attacked surface which revealed features like those in Fig. 10. In some cases a film of material obscured the feature, and in other cases, colours provided enhancement of contrast. Attempts to show that the features in Fig. 10 might be due to contraction of a swollen surface layer proved to be inconclusive. Slow cooling, water quenching and liquid nitrogen quenching of the etched article immediately after removal from the etching fluid did not produce consistent variation

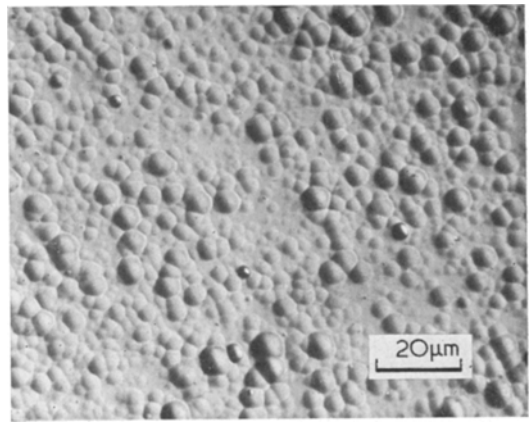

Figure 9 Fracture surface etched 1 h at 95°C in CrO_3/H_2O. Reflected light micrograph. Cast 16, 30 parts DDM.

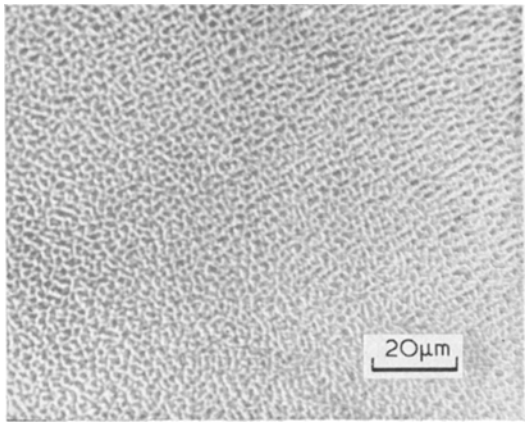

Figure 10 Fracture surface etched 1 h at 95°C in CrO_3/H_2SO_4/H_3PO_4/H_2O. Reflected light micrograph. Cast 16, 30 parts DDM.

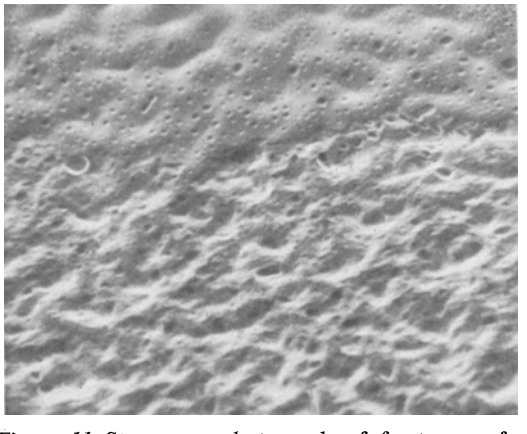

Figure 11 Stereoscan photograph of fracture surface etched for 1 h in CrO_3/H_2SO_4/H_3PO_4/H_2O. Cast 14, 27 parts DDM × 7500.

in the size of the feature. Stereoscan observation of the etched surfaces revealed the presence of craters and hillocks but did not serve to prove one way or the other that the etched surface was comprised of structural features (Fig. 11). The result shown in Fig. 9 was consistently achieved by CrO_3/H_2O etching, and the only difference between the various resin mixes was a difference in the time taken to achieve complete coverage of the surface with the features shown. The 20 and 40 parts DDM resins took approximately the same time to get to this condition, whereas the intermediate mixtures took longer. There was no apparent difference in the final result, however, Fig. 9 typifying all resin compositions. The propagation of cracks through etched specimens indicated that the feature shown in Fig. 9 did not influence the movement of the crack, at least not in the fast propagation zone.

4.5. Small angle X-ray scattering

Small angle X-ray studies [21] produced no significant scattering in any of the resins of 20, 27, 30 and 40 parts DDM. (35 parts was not investigated.) The obvious implication is that the resins do not behave as a two-phase structure containing a significant proportion of one phase having a particle size in the 50 Å to 1000 Å range. This does not, of course, rule out the possibility of a larger structural unit.

4.6. General comments on above results

The fracture data are in accordance with expectations as far as the methods of evaluation of γ is concerned. It is reasonable that the two analytical methods (Berry's and Irwin-Kies' equations) should agree more closely because they employ data from equivalent situations. The averaging caused by the area under the load-extension curve method, and the fact that the "area" figure is below the initiation figures at all compositions means that care must be taken when interpreting area-under-curve results or comparing them with those for other materials whose crack-jumping tendency and rate-sensitivity of FSE may be grossly different. There was considerable discrepancy between results obtained by Berry's method and Irwin-Kies' equation at 35 parts DDM. Large crack jumps were prevalent at this composition and this limited the amount of test data available from each specimen. Consequently, the result is less reliable statistically.

The mechanical behaviour of the various resin compositions is surprising. For example, the modulus trend is not easily explained, in terms of cross-link density, in the range 20 to 27 parts DDM. Why should an increase in DDM content (and presumably in cross-link density) result in a decrease in modulus? (It is considered by the authors that an investigation into the network structure at the gel point may lead to an explanation of such apparently anomalous behaviour.

Transition temperatures, on the other hand, are in agreement with the concept of maximum crosslink density at Stoichiometry with effective lowering of crosslink density on either side of the 100/27:828/DDM ratio. This may be for one of the following reasons:

(a) insufficient crosslink agent on the low side

of the stoichiometric DDM content i.e. the presence of uncured resin

(b) the presence of unreacted DDM or partially reacted Epikote 828 and DDM.

A check on the degree of cure of the nominally stoichiometric resin mixes was carried out by extending the post cure stage (see Table I) at 175°C by up to 1.6 h. The results were such that no significant differences, in any measured property, were obtained in comparison with the stoichiometric mix which was post-cured for the nominal 2 h at 175°C. It is suggested that the post cure heat treatment originally employed was sufficient to complete the reaction as far as physically possible in the 100/27:828/DDM system gelled at 100°C. A change in gel temperature would clarify the situation with respect to extent of cure.

Tests at crosshead speeds of 1.0 and 10.0 mm min^{-1} in stoichiometric resin revealed a decrease in γ as speed increased. FSE determined by the Irwin-Kies equation was more sensitive to testing speed than FSE obtained from the area-under-curve method. A decrease in K_{IC} was also observed and an increase in Young's modulus was evident. Measurements of rough-zone sizes at various testing speeds were also made for this resin mix. A decrease in rough zone size was noted (see Table IV).

Chemical etching of epoxies has been carried out previously by Cuthrell [22]. His work suggests that the curing epoxy has a colloidal nature, and that the resulting crosslinked mass retains some of the essential features of a two-phase structure, i.e. a dense floccular phase dispersed in a matrix of less dense material which resembles the uncured resin. Furthermore, the implication is that a regular arrangement of floccules is obtained. If this is so, it is reasonable to suppose that such a two-phase structure would influence mechanical and fracture properties. It should be pointed out that Cuthrell's investigations were on a polyol-modified Epon 828 cured with an anhydride. It may be that such a system lends itself to colloidal behaviour. All the evidence from present work on unmodified Epikote 828/DDM systems suggests that no such two-phase structure exists. Therefore, one has to look for explanations for the variation in mechanical and fracture properties in other areas. At present, it is only possible to state which lines of approach have proved to be unsuccessful in respect of elucidating any structural explanation for the variations reported. It is obvious, however, that toughening occurs as the DDM content is increased up to approximately 35 parts DDM and that the stoichiometric compound is not necessarily synonymous with optimum fracture properties. It may be that DDM in excess of approximately 27 parts acts as a plasticising agent with regard to crack tip processes, allowing considerable blunting prior to catastrophic failure of the whole specimen. The reason for material with more than 35 parts DDM becoming less tough may be associated with the concept of decreasing crosslink density because of "extension" by the excess hardener, by chemical and/or physical means. While treatment of the results by a Dugdale type model [23] may provide a better understanding of the crack tip plasticity aspects of the problem, at present, effort is being focused on the microscopic aspects of the problem. It is hoped that a link between the bulk properties and the mechanics of the crosslinking reactions can be achieved in the near future.

5. Conclusions

5.1. The method of evaluating fracture parameters for comparative purposes must be compatible with the mode of propagation of the crack and the specific nature (and intended use) of the parameter involved. Points to consider are whether the data refers to initiation, propagation, or arrest values, especially for materials with a high tendency to fail by crack jumping (stick-slip) mechanisms.

5.2. In the system Epikote 828/Epikure DDM, cured (nominally) 1 h at 100°C + 2 h at 175°C, a peak in the FSE (γ) and K_{IC} versus DDM content curves is found at approximately 35 parts DDM. The reasons for this are not clear and the simple concept of cross-link density alone cannot explain the variation. Considerable crack blunting occurs in resins of stoichiometric DDM content (and above this level of DDM). This is not the case for low DDM content material. There is also a difference in crack tip morphology for the low DDM content material at the extremes of a crack jump.

5.3. Tensile and compressive modulus, compressive yield stress and compressive 1% proof stress all show a minimum at 27 parts DDM. At present there is no explanation for this variation although the investigation of network parameters may provide an answer.

5.4. Fracture and mechanical properties of Epikote 828/Epikure DDM are slightly rate

sensitive in the range of crosshead speeds 0.1 to 10.0 mm min^{-1}. In particular, fracture surface energy and plane strain fracture toughness show a slight decrease with increase in testing speed.

6. Appendix

In order to compare the behaviour of the practical fracture toughness specimens with theoretical expectations and to compare the three methods of evaluating FSE, it was decided that the test data be analysed both statistically and by a manual graphical method. Average values of FSE were obtained by treating the test data in the following ways:

TABLE A I Comparison of FSE results obtained by statistical (all data and selected data) methods and by manual graph plotting – individual specimens

	Irwin-Kies equation		Number of specimens for mean calculation		Berry's equations		
Cast number	Mean γ (J m^{-2})	Standard error	(Irwin-Kies)	(Berry)	Mean γ (J m^{-2})	Standard error	Text paragraph reference
Statistical line-fitting							
15	68.2	2.9(7)	5	5	70.5	4.7	6.1.
17	67.8	3.0	5	5	65.8	4.1	6.2.
21							
12	206.1	2.9(5)	5	6	250.3	14.9	6.1.
13	203.3	2.4(5)	5	6	250.3	14.9	6.2.
14							
16	405.2	27.2	4	4	394.0	18.6	6.1.
18	342.8	8.3	4	4	368.5	32.1	6.2.
Manual line-fitting							
15							
17	69.9	2.1	5	5	70.6	2.5	—
21							
12							
13	202.1	2.2	5	6	233.7	16.3	—
14							
16	340.3	7.9	4	4	416.5	25.9	—
18							

Mean values are means of γ values obtained from individual specimens.

TABLE A II Comparison of FSE results obtained by statistical (all data) methods and by manual graph plotting – "combined" specimens

	Berry's equations			Irwin-Kies equation				
Cast number	Correlation coeff. of $\log f/\delta$ versus $\log C$ plot	Correlation coeff. of $f\delta/w$ versus C plot	γ (J m^{-2})	Correlation coeff. of R versus C plot	γ (J m^{-2})	γ by Berry's method (J m^{-2})	γ by Irwin-Kies equation (J m^{-2})	Number of specimens
	Statistical line-fitting			*Statistical line-fitting*		*Manual line-fitting*		
15								
17	0.9889	0.9654	72.9	0.9972	70.5	88.4	61	5
21								
12								
13	0.8598	0.9072	197.2	0.99	205.6	191.2	200	5
14								
16	0.9995	0.9889	396	0.9977	391.9	308–362	344	4
18								
19	0.9998	0.9455	787	0.9981	514.9	880	514	2
20	0.9996	0.9874	275	0.9976	200.4	299	212	2

6.1. *All* fracture test data points from *individual* specimens were fitted to straight lines (by the least squares method) for the Berry and Irwin-Kies analyses. This allowed a value of γ to be obtained for each test specimen. The results were compared with values of FSE obtained by manually plotting the various graphs for each specimen.

6.2. *Selected* test data points from individual specimens were fitted to straight lines by the least squares method. Selection of data was achieved by ignoring figures appertaining to very short (< 30 mm) or very long (> 120 mm) crack lengths where the desired constancy of the dR/dC term in the Irwin-Kies equation is least likely to be found. The results were compared with those from 6.1. The same criterion of selection was used for the data treated by Berry's equations. (A comparison with manually plotted data of Section 6.1 can also be made.)

6.3. *All* fracture test data points from *all like-specimens* were fitted to "combined" straight lines by the least squares method. The resulting value of FSE for each set of like-specimens was compared with the values obtained by methods outlined in sections 6.1 and 6.2. Manual graph plotting of "combined" straight lines was also done. The results of analyses 6.1 and 6.2 are shown in Table AI. The results for the analysis 6.3 are summarized in Table AII.

It can be argued that it is inherently better to consider individual specimens, so that variations from cast to cast and test to test are realistically included in the result. This is so, provided that adequate data can be generated from a single test. Since most of the resin systems investigated exhibited a stick-slip mode of crack propagation, with fairly large crack-jumps (under the prevailing test conditions), it can also be argued that case 6.3 is likely to provide a more realistic average, if batch and test variations are shown to be small.

The main conclusions from a study of Tables AI and AII are

(a) As specimen FSE increases, the error in the result tends to increase. This is most likely to be the result of having fewer crack arrest points per specimen in the case of the tough resins, combined with the fact that only two specimens from casts 19 and 20 were tested. In fact, only "combined" results for these casts were considered realistic because of the comparative lack of data. This is one reason for using results from "combined" plots in Fig. 3.

(b) Generally, there is little scatter in the results, regardless of the method of plotting, except at the toughest resin compositions (casts 19 and 16 in particular).

(c) Differences between the resins based on FSE calculations are significant.

Acknowledgements

Thanks are due to the following for their help in the acquisition of the information reported in this paper: The Science Research Council, for financial support, in the form of a Research Studentship (K.S.); Dr D. S. Brown (Chemistry Department, Loughborough University of Technology) for small angle X-ray data; Dr A. Meeks (Shell Research Laboratories, Egham) for advice on the casting and curing of epoxy resins and for several helpful discussions; Shell Chemical Company Limited, for providing raw materials; and Mr K. Ellison, (Department of Materials Technology, Loughborough University of Technology), for helpful discussions on design of apparatus and for manufacture of same.

References

1. R. GRIFFITHS, M.Sc. Thesis, University of Keele (1968).
2. A. D. S. DIGWAA, *Polymer* **15** (1974) 101.
3. T. KOBAYASHI, Ph.D. Thesis, Illinois Institute of Technology, (May 1972).
4. G. P. MARSHALL, L. E. CULVER and J. G. WILLIAMS, *Plastics and Polymers* (February 1969) 75.
5. J. P. BERRY, *J. Appl. Phys.* **34** (1963) 62.
6. G. R. IRWIN and J. A. KIES, *Welding Journal Research Supplement* **33** (1954) 193s.
7. C. GURNEY, "Physical Basis of Yield and Fracture" (Oxford, Conference, 1966).
8. L. E. MILLER, K. E. PUTTICK and J. G. RIDER, *J. Polymer Sci.* **33c** (1971) 13.
9. P. P. GILLIS and J. J. GILMAN, *J. Appl. Phys.* **35** (1964) 647.
10. J. W. OBREIMOV, *Proc. Roy. Soc.* **A127** (1930) 290.
11. J. J. GILMAN, Fracture – Proceedings of an International Conference on atomic mechanisms of fracture, Swampscott, Mass. (Wiley, USA, 1959).
12. *Ibid*, "Fracture", edited by J. Averbach *et al.* (Wiley, 1956).
13. J. J. BENBOW and F. C. ROESLER, Proceedings of Physical Society **B70** (1957) 201.
14. J. P. BERRY, *J. Mech. Phys. Sol.* **8** (1960) 194.
15. R. G. HOAGLAND, *J. Basic Eng.* (September, 1967).
16. R. J. FERGUSON and J. G. WILLIAMS, *Polymer* **14** (1973) 103.
17. S. MOSTOVOY, B. P. CROSSLEY and E. J. RIPLING, Materials Research Lab. Inc. (June 1966).
18. J. G. WILLIAMS, *Int. J. Fract. Mech.* **8** (1972) 393.

19. R. GRIFFITHS and D. G. HOLLOWAY, *J. Mater. Sci.* **5** (1970) 302.
20. M. J. DOYLE, *et al.*, *Proc. Roy. Soc.* **A329** (1972) 137.
21. R. N. HAWARD, (Ed.), "The Physics of Glassy Polymers", (Applied Science Publishers, London, 1973) p. 130.
22. R. E. CUTHRELL, *J. Appl. Polymer Sci.* **12** (1968) 1263.
23. D. S. DUGDALE, *J. Mech. Phys. Sol.* **8** (1960) 100.

Received 29 April and accepted 12 July 1974.